Sparse Array Channel Estimation for Subarray-Based Hybrid Beamforming Systems

Joerg Eisenbeis, *Graduate Student Member, IEEE*, Nicolai Kern, *Graduate Student Member, IEEE*, Magnus Tingulstad, Lucas Giroto de Oliveira, *Graduate Student Member, IEEE*, and Thomas Zwick, *Fellow, IEEE*

***Abstract*—Subarray-based hybrid beamforming communication systems are a cost- and power-efficient architectural solution to realize massive multiple-input multiple-output (MIMO) systems. To estimate the required channel state information (CSI) current research focuses on beam training algorithms, which suffer from long estimation times and require precise system calibration. In order to overcome these problems, two channel estimation algorithms in combination with suitable beamforming algorithms are proposed. The presented algorithms are based on sparse array measurements, where only one antenna per subarray is active during the estimation process. This allows for the reconstruction of the complex MIMO channel matrix by performing multiple sparse array measurements. Channel estimation algorithms, which drastically reduce the channel estimation time are proposed in this letter. Their high performance is proven in small cell communication measurements around 28 GHz.**

***Index Terms*—Channel estimation, MIMO communication, mobile communication.**

I. Introduction

HYBRID beamforming systems split the beamforming process into a digital and analog beamforming network enabling a cost and energy-efficient implementation of massive multiple-input multiple-output (MIMO) communication systems [1]. An especially efficient architectural realization of the analog beamforming network is the subarray-based (also denominated as *sub-connected* or *partially-connected*) hybrid beamforming architecture [2]. Thereby the analog beamforming network connects each digital channel to a subarray of antenna elements via a dedicated phase shifter. One of the main challenges of subarray-based hybrid beamforming systems is the acquisition of the channel state information (CSI). Current research on channel estimation for hybrid beamforming systems in the centimeter-wave (cmWave) and millimeter-wave (mmWave) region focuses on beam training algorithms. These algorithms try to find the dominant spatial propagation paths characterized by pairs of angles of departure (AoDs) at the transmitter (Tx) and angles of arrival (AoAs) at the receiver (Rx). To decrease the estimation time of an exhaustive search the works presented in [3]–[9] adopt hierarchical codebook-based approaches. These hierarchical beam training algorithms divide the search process into different subsequent codebook levels, where at first the full angular range is scanned using wide sector beam patterns [4]. Unfortunately, the architectural constraints of the subarray-based hybrid beamforming architecture make the generation of wide sector beam patterns difficult. Moreover, system calibration in amplitude and phase is required to steer the beam in the desired angular direction [10]. Beside the hierarchical beam training algorithms, the sparse nature of the channel can be exploited at higher mmWave frequencies by utilizing compressed sensing techniques [11]–[16]. This leads to a decrease in training overhead but assumes a sparse channel with only a few spatial propagation paths.

In this letter two novel channel estimation algorithms are proposed for subarray-based hybrid beamforming architectures based on sparse array measurements. The focus is on the new radio n257-band around 28 GHz specified by the 3rd generation partnership project (3GPP). In this band the presented measurements by Rappaport *et al.* [17] show an average of 4.7 multipath components between a transmitter and a receiver. As a result, compressed sensing techniques as presented in [11], considering only one spatial path between the transmitter and receiver, are not applicable. Moreover, the proposed algorithms aim to reduce the long estimation times of current beam training algorithms.

This letter is structured as follows: First, the sparse array channel estimation concept as well as the algorithms are presented in Section II. The reduction of the estimation time compared to an exhaustive search is derived in Section III. Finally, the high performance of the algorithms is demonstrated in Section IV by means of MIMO outdoor communication measurements around 28 GHz.

II. Sparse Array Channel Estimation Approach

Subarray-based hybrid beamforming systems connect each digital channel with a dedicated number of antenna elements. The number of antennas per subarray results to $N_{\mathrm{sub}} = N_{\mathrm{ant}}/N_{\mathrm{dig}}$, where N_{ant} represents the total number of antenna elements and N_{dig} denotes the number of digital channels, i.e., the number of subarrays. To reduce the hardware effort in the digital domain, the number of antennas is in general chosen

Manuscript received July 30, 2020; accepted September 12, 2020. Date of publication September 18, 2020; date of current version February 9, 2021. This work was supported in part by the Electronic Components and Systems for European Leadership Joint Undertaking Funded under H2020-EU.2.1.1.7. in Frame of the TARANTO Project under Grant ID 737454, and in part by the German Federal Ministry of Education under Grant 16ESE0211. The associate editor coordinating the review of this article and approving it for publication was C. Huang. *(Corresponding author: Joerg Eisenbeis.)*

The authors are with the Institute of Radio Frequency Engineering and Electronics, Karlsruhe Institute of Technology, 76131 Karlsruhe, Germany (e-mail: joerg.eisenbeis@kit.edu).

Digital Object Identifier 10.1109/LWC.2020.3025171

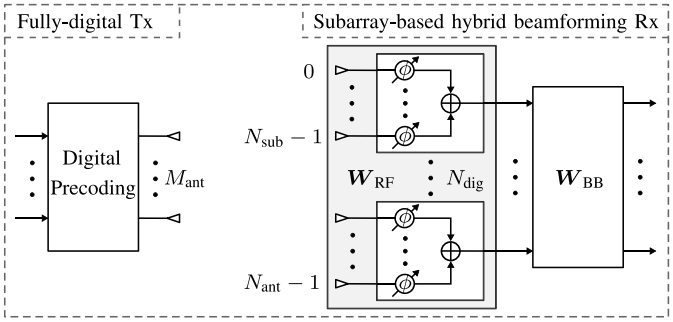

Fig. 1. Block diagram of the considered uplink communication scenario with a fully digital transmitter and a subarray-based hybrid beamforming Rx.

much larger than the number of digital channels, such that $N_{\text{ant}} \gg N_{\text{dig}}$. The beamforming matrix at the Rx results to $\boldsymbol{W} = \boldsymbol{W}_{\text{RF}} \cdot \boldsymbol{W}_{\text{BB}}$, where the analog beamforming matrix of block-diagonal form is denoted $\boldsymbol{W}_{\text{RF}} \in \mathbb{C}^{N_{\text{ant}} \times N_{\text{dig}}}$ and the digital beamforming matrix is written as $\boldsymbol{W}_{\text{BB}} \in \mathbb{C}^{N_{\text{dig}} \times N_{\text{dig}}}$. Due to the hardware constraint introduced by the analog beamforming network the antenna elements of one subarray can no longer be distinguished in the digital domain.

A. Sparse Array Measurement

For the sparse array measurement only one antenna element per subarray is activated at a time [18]. This allows a separation of the remaining active antenna elements in frequency, time or signal domain. In this letter, the signals of the Tx antennas are separated by using different interleaved orthogonal frequency division multiplexing (OFDM) subcarriers. OFDM is chosen as multicarrier scheme due to its robustness against frequency-selective fading and as it is currently considered by 3GPP in release 15 as part of the first phase of the fifth generation of mobile communication (5G) [19]. For the sake of clarity, we simplify our considerations without loss of generality to an uplink communication scenario between a fully digital MIMO Tx and a subarray-based hybrid beamforming Rx. This restriction is motivated by the fact that space is limited in mobile devices and thus a very large number of antennas will not be integrated in the near future, making a fully digital architecture preferable. The selected scenario is also consistent with the measurement-based analysis presented later. A block diagram of the considered scenario is depicted in Fig. 1.

For an OFDM-based data transmission the N_{c} OFDM subcarriers containing the training data can be addressed by the index set $\mathcal{C} \in \{0, 1, \ldots, N_{\text{c}} - 1\}$. This index set is divided into M_{ant} subsets $\mathcal{C}_m \subseteq \mathcal{C}$ with $m \in \{0, 1, \ldots, M_{\text{ant}} - 1\}$, where

$$\mathcal{C} = \dot{\bigcup}_{m=1}^{M_{\text{ant}}} \mathcal{C}_m \tag{1}$$

holds, realizing the separation of the transmit antennas by different OFDM subcarriers. Thereby $\dot{\bigcup}$ denotes for the disjoint union. The discrete time-domain OFDM signal with sampling times $t = \xi \cdot T_{\text{o}}/N_{\text{c}}$ and $\xi \in \{0, 1, \ldots, N_{\text{c}} - 1\}$ can be written as [20]

$$\boldsymbol{u}(m, \xi) = \sum_{p=0}^{N_{\text{c}}-1} \boldsymbol{X}(m, p) \cdot e^{j2\pi p \xi / N_{\text{c}}}, \tag{2}$$

where T_{o} represents the OFDM symbol duration, m the indices for the M_{ant} transmit antennas and $p \in \{0, 1, \ldots, N_{\text{c}} - 1\}$ the indices for the OFDM subcarrier frequencies

$$f_p = p \cdot \Delta f = p / T_{\text{o}} \tag{3}$$

with the subcarrier spacing $\Delta f = B_{\text{s}}/N_{\text{c}}$ and signal bandwidth B_{s}. The index set addressing the antenna elements of the subarray-based hybrid beamforming Rx $\mathcal{I} \in \{0, 1, \ldots, N_{\text{ant}} - 1\}$ can be divided in subsets of indices $\mathcal{I}_d \subseteq \mathcal{I}$ with $d \in \{1, 2, \ldots, N_{\text{dig}}\}$, where $\mathcal{I}_d$ contains the N_{sub} indices of the d-th subarray. For the sparse array measurement exactly one antenna per subarray is active at a time. The selection of active antennas can be addressed by the index set $\mathcal{I}_{\text{s}} \subseteq \mathcal{I}$, where $\mathcal{I}_{\text{s}}$ contains one element of each of the subsets $\mathcal{I}_d$. The elements of $\mathcal{I}$, $\mathcal{I}_d$, and $\mathcal{I}_{\text{s}}$ are the absolute antenna indexes. For a selected sparse array constellation $n \in \mathcal{I}_{\text{s}}$ the received signal in time domain $\boldsymbol{y} \in \mathbb{C}^{N_{\text{dig}} \times N_{\text{c}}}$ results to

$$\boldsymbol{y}(n, \xi) = \sum_{m=0}^{M_{\text{ant}}-1} \boldsymbol{h}(n, m, \xi) * \boldsymbol{u}(m, \xi) + \boldsymbol{n}(n, \xi), \tag{4}$$

where $\boldsymbol{h} \in \mathbb{C}^{N_{\text{dig}} \times M_{\text{ant}} \times N_{\text{c}}}$ represents the complex channel matrix and $\boldsymbol{n} \in \mathbb{C}^{N_{\text{dig}} \times N_{\text{c}}}$ accounts for the additive white Gaussian noise (AWGN) introduced during transmission. After Fourier transformation the received signal in frequency domain $\boldsymbol{R} \in \mathbb{C}^{N_{\text{dig}} \times N_{\text{c}}}$ results to

$$\boldsymbol{R}(n, p) = \sum_{m=0}^{M_{\text{ant}}-1} \boldsymbol{H}_{\text{s}}(n, m, p) \boldsymbol{X}(m, p) + \boldsymbol{N}(n, p), \tag{5}$$

assuming that the coherence time is longer than the OFDM symbol duration, where $\boldsymbol{H}_{\text{s}} \in \mathbb{C}^{N_{\text{dig}} \times M_{\text{ant}} \times N_{\text{c}}}$ represents the channel frequency response and $\boldsymbol{N} \in \mathbb{C}^{N_{\text{dig}} \times N_{\text{c}}}$ the additive white Gaussian noise in frequency domain. At the Rx the channel can be estimated using least squares estimation [21]

$$\hat{\boldsymbol{H}}_{\text{s,f}}(n, p) = \boldsymbol{R}(n, p) \cdot \boldsymbol{T}(p)^{-1}, \tag{6}$$

with the known transmit data symbols

$$\boldsymbol{T}(p) = \sum_{m=0}^{M_{\text{ant}}-1} \boldsymbol{X}(m, p). \tag{7}$$

As the transmitters are separated by their OFDM subcarriers defined in $\mathcal{C}_m$ the MIMO channel matrix can be estimated to

$$\hat{\boldsymbol{H}}_{\text{s}}(n, m) = \frac{1}{|\mathcal{C}_m|} \sum_{p \in \mathcal{C}_m} \hat{\boldsymbol{H}}_{\text{s,f}}(n, p), \tag{8}$$

averaging over all subcarriers of each transmitter assuming a frequency non-selective channel over the full signal bandwidth. The result is the complex MIMO channel matrix $\hat{\boldsymbol{H}}_{\text{s}} \in \mathbb{C}^{N_{\text{dig}} \times M_{\text{ant}}}$.

Algorithm 1 Multiple Sparse Array Measurements (MSAM)

1: **Input:** $\mathcal{I}_{\mathrm{s},\,i}$ with $i \in \{0, \ldots, N_{\mathrm{sub}} - 1\}$
2: **for** $0 \leq i \leq (N_{\mathrm{sub}} - 1)$
3: Sparse array measurement with $\mathcal{I}_{\mathrm{s},\,i} \rightarrow \hat{\boldsymbol{H}}_{\mathrm{s},\,i}$
3: Reshape $\hat{\boldsymbol{H}}_{\mathrm{s},\,i}$ using (9)
4: **end**
5: Reconstruct $\hat{\boldsymbol{H}}$ using (10)
6: Calculate $\boldsymbol{W}$ using SIC algorithm
7: **Output:** $\boldsymbol{W} \in \mathbb{C}^{N_{\mathrm{ant}} \times N_{\mathrm{dig}}}$

B. Multiple Sparse Array Measurements

The *Multiple Sparse Array Measurements* (MSAM) algorithm is a simple approach to reconstruct the full MIMO channel matrix $\hat{\boldsymbol{H}} \in \mathbb{C}^{N_{\mathrm{ant}} \times M_{\mathrm{ant}}}$. The channel matrix is reconstructed by performing N_{sub} subsequent channel measurements with different sparse array constellations [18].

The estimation result for each of the $i \in \{0, \ldots, N_{\mathrm{sub}} - 1\}$ subsequent sparse array measurements can be described by a matrix $\hat{\boldsymbol{H}}_i \in \mathbb{C}^{N_{\mathrm{ant}} \times M_{\mathrm{ant}} \times N_{\mathrm{sub}}}$ constructed by

$$\hat{\boldsymbol{H}}_i(n, \cdot, i) = \begin{cases} \hat{\boldsymbol{H}}_{\mathrm{s},\,i}, & n = \mathcal{I}_{\mathrm{s},\,i} \\ 0, & \text{else.} \end{cases} \tag{9}$$

The sparse array estimation result $\hat{\boldsymbol{H}}_i(\cdot, \cdot, i)$ contains at the sampling times $t = i \cdot T_{\mathrm{e,s}}$ only $N_{\mathrm{dig}} \cdot M_{\mathrm{ant}}$ non-zero entries at the row indices $\mathcal{I}_{\mathrm{s},\,i}$, where $T_{e,s}$ represents the sparse array estimation time. The row indices $\mathcal{I}_{\mathrm{s},\,i}$ thereby represent the active Rx antennas. The different constellations $\mathcal{I}_{\mathrm{s},\,i}$ are chosen to satisfy $\mathcal{I} = \dot{\cup}_{i=0}^{N_{\mathrm{sub}}-1} \mathcal{I}_{\mathrm{s},\,i}$ and $\cap_{i=0}^{N_{\mathrm{sub}}-1} \mathcal{I}_{\mathrm{s},\,i} = \varnothing$ holds. The full MIMO channel matrix is reconstructed by summing up the N_{sub} subsequent measurements resulting in

$$\hat{\boldsymbol{H}} = \textstyle\sum_{i=0}^{N_{\mathrm{sub}}-1} \hat{\boldsymbol{H}}_i(\cdot, \cdot, i). \tag{10}$$

Based on the reconstructed full channel matrix we calculate the beamforming matrix $\boldsymbol{W}$ at the Rx using the Successive Interference Cancellation (SIC) algorithm presented by Gao *et al.* in [22]. The pseudo-code for the MSAM algorithm is shown in **Algorithm 1**.

C. Sparse Array Beam Analysis

In contrast to the MSAM algorithm, the *Sparse Array Beam Analysis* (SABA) algorithm tries to identify the main propagation directions, analyzing the estimated sparse array channel matrix $\hat{\boldsymbol{H}}_{\mathrm{s}}$. Starting from the singular value decomposition (SVD) result of the sparse array matrix $\hat{\boldsymbol{H}}_{\mathrm{s}} = \boldsymbol{U}_{\mathrm{s}} \boldsymbol{\Sigma}_{\mathrm{s}} \boldsymbol{V}_{\mathrm{s}}^{H}$, where $\boldsymbol{U}_{\mathrm{s}} \in \mathbb{C}^{N_{\mathrm{dig}} \times N_{\mathrm{dig}}}$ and $\boldsymbol{V}_{\mathrm{s}} \in \mathbb{C}^{M_{\mathrm{ant}} \times M_{\mathrm{ant}}}$ represent unitary matrices and $\boldsymbol{\Sigma}_{\mathrm{s}} \in \mathbb{C}^{N_{\mathrm{dig}} \times M_{\mathrm{ant}}}$ donates for a diagonal matrix containing the singular values of $\hat{\boldsymbol{H}}_{\mathrm{s}}$, the beamforming matrix at the Rx is selected as $\boldsymbol{W}_s = \boldsymbol{U}_{\mathrm{s}}^{H}$. For better clarity, in the following steps of the algorithm a linear array is considered. However, the described algorithm can be easily extended for planar arrays. At the Rx the beam pattern in azimuth φ is calculated for the beamforming matrix $\boldsymbol{W}_s \in \mathbb{C}^{N_{\mathrm{dig}} \times N_{\mathrm{dig}}}$ by

$$\boldsymbol{C}_{\mathrm{s}}(\varphi) = \sum_{r=0}^{N_{\mathrm{dig}}-1} \left| \sum_{n=0}^{N_{\mathrm{dig}}-1} \boldsymbol{W}_{\mathrm{s}}(n, r)\, \boldsymbol{C}_{\mathrm{e}}(n, \varphi) e^{jk\vec{d}(n)\sin\varphi} \right| \tag{11}$$

Algorithm 2 Sparse Array Beam Analysis (SABA)

1: **Input:** $\mathcal{I}_{\mathrm{s}}$
2: Sparse array measurement with $\mathcal{I}_{\mathrm{s}} \rightarrow \hat{\boldsymbol{H}}_{\mathrm{s}}$
3: Define $\boldsymbol{W}_s = \boldsymbol{U}_{\mathrm{s}}^{H}$ with $\hat{\boldsymbol{H}}_{\mathrm{s}} = \boldsymbol{U}_{\mathrm{s}} \boldsymbol{\Sigma}_{\mathrm{s}} \boldsymbol{V}_{\mathrm{s}}^{H}$
4: Calculate $\boldsymbol{C}_{\mathrm{s}}(\varphi)$ using (11)
5: Find local maximas $\vec{v}_s \in \mathbb{R}^{N_d \times 1}$ in $\boldsymbol{C}_{\mathrm{s}}(\varphi)$ above threshold Γ
6: **for** $1 \leq i \leq N_d$
7: Select ϕ fulfilling $\min_{\phi}\{|\vec{v}_{\phi} - \vec{v}_s(i)|\}$
8: Beam steering towards $\vec{a}(\phi)$ (with (12))
9: Measure the received power $\vec{P}_{\mathrm{Rx}}(i)$
10: **end**
11: Select the N_{dig} largest indices $\vec{\kappa}$ evaluating $\vec{P}_{\mathrm{Rx}}$
12: Construct $\boldsymbol{W}$ with the $\vec{v}_s(\vec{\kappa}(m))$ for $m \in \{1, \ldots, N_{\mathrm{dig}}\}$
13: **Output:** $\boldsymbol{W} \in \mathbb{C}^{N_{\mathrm{ant}} \times N_{\mathrm{dig}}}$

where $\boldsymbol{C}_{\mathrm{e}}$ contains the antenna element characteristics, $k = 2\pi/\lambda$ denotes the wave number, and $\vec{d}$ represents a vector with the spatial positions of the active antenna elements. The dominant AoAs are then identified by searching for the local maxima in $\boldsymbol{C}_{\mathrm{s}}(\varphi)$. The angular vector of the N_d detected maxima $\vec{v}_s = [\varphi_1, \ldots, \varphi_{N_d}]$ is in addition limited by a threshold Γ with respect to the global maximum $\max\{\boldsymbol{C}_{\mathrm{s}}(\varphi)\}$. As the large antenna spacing of the active antennas for the sparse array measurement leads to grating lobes within the antenna array characteristic, ambiguities for the main propagation directions are present in the beam pattern $\boldsymbol{C}_{\mathrm{s}}(\varphi)$. These ambiguities are filtered out in the second phase of the SABA algorithm by using directive beams. The full antenna array is pointed subsequently towards each element of $\vec{v}_{\mathrm{s}}$ to identify the real propagation paths by observing the received power. The directional beams are selected from the exhaustive search codebook with the array response vectors [8]

$$\vec{a}(\phi) = \frac{1}{\sqrt{N_{\mathrm{ant}}}} \left[1, e^{jkd_{\mathrm{a}}\sin\phi}, \ldots, e^{jkd_{\mathrm{a}}(N_{\mathrm{ant}}-1)\sin\phi}\right] \tag{12}$$

where the possible beam steering angles $\vec{v}_{\phi} \in \{, \ldots, -2\phi_r, -\phi_r, 0, \phi_r, 2\phi_r, \ldots, \}$ are considered to be limited by the phase shifter resolution q resulting in

$$\phi_r = \arcsin\left\{\frac{\lambda}{d_{\mathrm{a}} \cdot 2^q}\right\}. \tag{13}$$

The beamforming matrix $\boldsymbol{W}$ is then constructed as described in a previous study [23], by steering each subarray towards one of the N_{dig} directions with the strongest received power. The pseudo-code for the SABA algorithm is shown in **Algorithm 2**.

In contrast to the MSAM algorithm, a calibration in amplitude and phase between the parallel Rx chains is needed. This calibration is also required for an exhaustive search and hierarchical beam training algorithms, as an uncalibrated system would lead to a distorted beam pattern. In general phase and amplitude imbalances between the parallel Rx chains are inevitable as they are caused by manufacturing tolerances of the circuit boards or RF components, differences in the temperature behavior of the components, and so forth.

TABLE I
COMPARISON OF THE REQUIRED ESTIMATION TIME

Estimation time	Exhaustive Search	MSAM	SABA
Formula (in T_m)	$\lceil \Psi/\psi_r \rceil$	$N_\mathrm{ant}^2/N_\mathrm{dig}$	$N_\mathrm{ant}+N_d$
This setup (in T_m)	67	64	23

III. ESTIMATION TIME ANALYSIS

The essential advantage of the proposed algorithms becomes clear by comparing the required estimation time. In order to put the estimation times of the presented algorithms into a relation, an exhaustive search is used as reference. The estimation time of an exhaustive search depends on the number of steering vectors within its codebook. With the limitations of the phase shifter resolution described by (13) and a confined angular coverage range in azimuth Φ the estimation time results to

$$T_\mathrm{e,exh} = \left\lceil \frac{\Phi}{\phi_r} \right\rceil \cdot T_\mathrm{m} = \left\lceil \frac{\Phi}{\arcsin\left\{ \frac{\lambda}{d_\mathrm{a} \cdot 2^q} \right\}} \right\rceil \cdot T_\mathrm{m}, \quad (14)$$

where T_m represents the measurement time for each beam steering angle of the exhaustive search codebook.

As the sparse array estimation utilizes no antenna array gain, the signal-to-noise ratio (SNR) is reduced by a factor corresponding to the numbers of antennas N_ant and has to be recovered for a fair comparison. Therefore the sparse array estimation time is enlarged to $T_\mathrm{e,s} = N_\mathrm{ant} \cdot T_\mathrm{m}$. It follows that the estimation time for the MSAM method results to

$$T_\mathrm{e,MSAM} = N_\mathrm{sub} \cdot T_\mathrm{e,s} = (N_\mathrm{ant}^2/N_\mathrm{dig}) \cdot T_m. \quad (15)$$

For the SABA algorithm, only one sparse array measurement is required, but in the second phase of the algorithm all possible angular directions have to be tested. The total estimation time for the SABA algorithm

$$T_\mathrm{e,SABA} = T_\mathrm{e,s} + N_d \cdot T_\mathrm{m} = (N_\mathrm{ant} + N_d) \cdot T_\mathrm{m} \quad (16)$$

therefore depends strongly on the number of angular directions N_d found by the sparse array measurements. Hence, that the threshold Γ has to be properly adjusted to balance the trade-off between the estimation time and the non-detection of individual spatial propagation paths. For our analysis, the threshold is set to $\Gamma = 0.1$ leading to an average of $N_d = 7$ detected angular directions. The estimation times for the presented MIMO measurement system are summarized in Table I with the system parameters $N_\mathrm{ant} = 16$, $N_\mathrm{dig} = 4$, $N_d = 8$, $d_\mathrm{a} = \lambda/2$, $q = 6$ bits, and $\Phi = 120°$.

IV. MEASUREMENT-BASED PERFORMANCE ANALYSIS

To analyze the performance of the presented channel estimation algorithms, the MIMO channel measurement system operating around 28 GHz presented in a previous work [24] is adopted. The measurements are performed in typical small cell site scenarios, where the base station is elevated on top of a building and the mobile Tx is placed at different spatial positions within the coverage area of the base station. For each of the in total 159 measurements the channel estimation is performed over 512 ms. This results in 4000 snapshots of the complex MIMO channel matrix.

TABLE II
UTILIZED SUBSEQUENT SPARSE ARRAY CONSTELLATION FOR THE MSAM ALGORITHM

i	0	1	2	3
$\mathcal{I}_{\mathrm{s},i}$	{1,5,9,13}	{2,6,10,14}	{3,7,11,15}	{4,8,12,16}

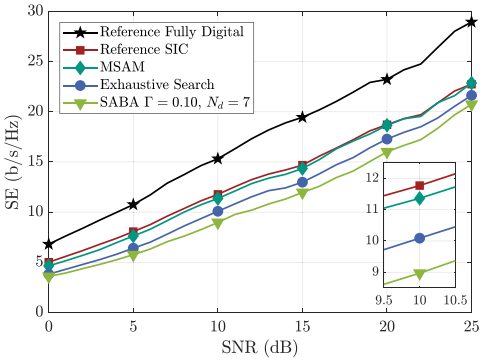

Fig. 2. SE over the SNR including all measurements.

The performance of the algorithms is compared by calculating the spectral efficiency [24]

$$\mathrm{SE} = \log_2\left\{ \left| \boldsymbol{I}_{N_\mathrm{ant}} + \frac{\gamma}{M_\mathrm{ant}} \boldsymbol{W}^H \boldsymbol{H} \boldsymbol{H}^H \boldsymbol{W} \right| \right\}, \quad (17)$$

assuming full CSI at the Tx, where $\boldsymbol{H}$ denotes the measured MIMO channel matrix, γ represents the SNR, and $\boldsymbol{I}_{N_\mathrm{ant}}$ denotes the identity matrix of dimension N_ant. The presented channel estimation algorithms consider a subarray size of $N_\mathrm{sub} = 4$ and consequently $N_\mathrm{dig} = 4$ digital channels. For the MSAM algorithm the active antenna constellations are given in Table II. The SABA algorithm employs the sparse array constellation given by $\mathcal{I}_\mathrm{s,BA} \in \{1, 5, 9, 16\}$ for the subsequent analysis.

To compare the algorithms, the measurements are ranked by the estimated SNR. For each SNR, a CDF of the SE with more than 4000 values is calculated and the 50% outage SE is determined. This enables to analyze the behavior of the performance for different SNRs regimes. As the measurement system uses a fully digital architecture, the SE of a 16×4 MIMO system can be calculated as an upper performance boundary.

For subarray-based hybrid beamforming architectures, the SE of the SIC algorithm serves as an upper performance boundary by assuming the knowledge of the full channel information at each point in time.

The results in Fig. 2 show that the SE of the MSAM algorithm is only slightly below the upper performance boundary for subarray-based hybrid beamforming architectures. This proves that the full MIMO channel matrix can be reconstructed by performing multiple subsequent sparse array measurements even with comparable long sparse array measurement times, here $T_\mathrm{m} = 128$ μs. Moreover, the high performance of the MSAM algorithm is proven by comparing it with the SE of the exhaustive search algorithm, which cannot reach the

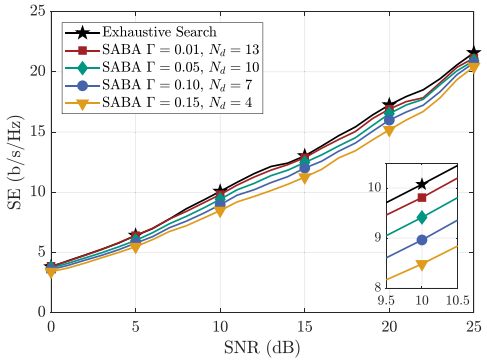

Fig. 3. SE over the SNR for different thresholds of the SABA algorithm.

performance of the MSAM algorithm. This is due to the better performance of the utilized beamforming algorithm for the MSAM approach. The SE of the SABA algorithm is slightly below the exhaustive search algorithm as the AoAs could not be as precisely detected by the reduced number of antennas. Note that for the exhaustive search and SABA algorithm the same beamforming algorithm is utilized after the AoAs are determined. However, the SABA algorithm drastically reduces the channel estimation time compared to the exhaustive search approach as shown in Table I.

The SE for different thresholds of the SABA algorithm is shown in Fig. 3. The presented results reveal the trade-off between the threshold and the estimation time. For a channel SNR of 10 dB, the loss in spectral efficiency compared to an exhaustive search is inegligible for very low threshold levels, i.e., $\Gamma \leq 0.01$. For a threshold level of $\Gamma = 0.15$, the loss increases to 1.5 b/s/Hz, but reduces the estimation time by roughly 30% compared to a threshold level of $\Gamma = 0.01$.

V. Conclusion

This letter presents two novel channel estimation algorithms for subarray-based hybrid beamforming systems. Employing multiple subsequent sparse array measurements allows a reconstruction of the full MIMO channel matrix, which enables the use of elaborated beamforming algorithms for subarray-based hybrid beamforming systems. Furthermore, no calibration of the amplitude and phase imbalances between the parallel Tx and Rx chains is required, as it has to be done for current beam training algorithms. The results show that the MSAM algorithm achieves a higher SE than the exhaustive search algorithm within a lower estimation time. The SABA algorithm allows to drastically reduce the estimation time and achieves dependent on the threshold level Γ nearly the performance of the exhaustive search algorithm.

References

[1] A. F. Molisch *et al.*, "Hybrid beamforming for massive MIMO: A survey," *IEEE Commun. Mag.*, vol. 55, no. 9, pp. 134–141, Sep. 2017.

[2] W. Roh *et al.*, "Millimeter-wave beamforming as an enabling technology for 5G cellular communications: Theoretical feasibility and prototype results," *IEEE Commun. Mag.*, vol. 52, no. 2, pp. 106–113, Feb. 2014.

[3] S. Hur, T. Kim, D. J. Love, J. V. Krogmeier, T. A. Thomas, and A. Ghosh, "Millimeter wave beamforming for wireless backhaul and access in small cell networks," *IEEE Trans. Commun.*, vol. 61, no. 10, pp. 4391–4403, Oct. 2013.

[4] A. Alkhateeb, O. E. Ayach, G. Leus, and R. W. Heath, "Channel estimation and hybrid precoding for millimeter wave cellular systems," *IEEE J. Sel. Topics Signal Process.*, vol. 8, no. 5, pp. 831–846, Oct. 2014.

[5] S. Noh, M. D. Zoltowski, and D. J. Love, "Multi-resolution codebook and adaptive beamforming sequence design for millimeter wave beam alignment," *IEEE Trans. Wireless Commun.*, vol. 16, no. 9, pp. 5689–5701, Sep. 2017.

[6] Z. Xiao, T. He, P. Xia, and X. G. Xia, "Hierarchical codebook design for beamforming training in millimeter-wave communication," *IEEE Trans. Wireless Commun.*, vol. 15, no. 5, pp. 3380–3392, May 2016.

[7] M. Kokshoorn, H. Chen, P. Wang, Y. Li, and B. Vucetic, "Millimeter wave MIMO channel estimation using overlapped beam patterns and rate adaptation," *IEEE Trans. Signal Process.*, vol. 65, no. 3, pp. 601–616, Feb. 2017.

[8] C. Lin, G. Y. Li, and L. Wang, "Subarray-based coordinated beamforming training for mmwave and sub-THz communications," *IEEE J. Sel. Areas Commun.*, vol. 35, no. 9, pp. 2115–2126, Sep. 2017.

[9] Y. Zhu, Q. Zhang, and T. Yang, "Low-complexity hybrid precoding with dynamic beam assignment in mmwave OFDM systems," *IEEE Trans. Veh. Technol.*, vol. 67, no. 4, pp. 3685–3689, Apr. 2018.

[10] T. Kühne and G. Caire, "An analog module for hybrid massive MIMO testbeds demonstrating beam alignment algorithms," in *Proc. 22nd Int. ITG Workshop Smart Antennas*, 2018, pp. 1–8.

[11] A. Alkhateeb, G. Leus, and R. W. Heath, "Compressed sensing based multi-user millimeter wave systems: How many measurements are needed?" in *Proc. IEEE Int. Conf. Acoust. Speech Signal Process. (ICASSP)*, Apr. 2015, pp. 2909–2913. [Online]. Available: https://ieeexplore.ieee.org/document/7178503

[12] X. Rao, V. K. N. Lau, and X. Kong, "CSIT estimation and feedback for FDD multi-user massive MIMO systems," in *Proc. IEEE Int. Conf. Acoust. Speech Signal Process. (ICASSP)*, vol. 62, May 2014, pp. 3157–3161.

[13] J. Lee, G.-T. Gil, and Y. H. Lee, "Channel estimation via orthogonal matching pursuit for hybrid MIMO systems in millimeter wave communications," *IEEE Trans. Commun.*, vol. 64, no. 6, pp. 2370–2386, Jun. 2016.

[14] S. Park and R. W. Heath, "Spatial channel covariance estimation for the hybrid MIMO architecture: A compressive sensing-based approach," *IEEE Trans. Wireless Commun.*, vol. 17, no. 12, pp. 8047–8062, Dec. 2018.

[15] X. Song, S. Haghighatshoar, and G. Caire, "A scalable and statistically robust beam alignment technique for millimeter-wave systems," *IEEE Trans. Wireless Commun.*, vol. 17, no. 7, pp. 4792–4805, Jul. 2018.

[16] Q. Qin, L. Gui, P. Cheng, and B. Gong, "Time-varying channel estimation for millimeter wave multiuser MIMO systems," *IEEE Trans. Veh. Technol.*, vol. 67, no. 10, pp. 9435–9448, Oct. 2018.

[17] T. S. Rappaport, G. R. MacCartney, M. K. Samimi, and S. Sun, "Wideband millimeter-wave propagation measurements and channel models for future wireless communication system design," *IEEE Trans. Commun.*, vol. 63, no. 9, pp. 3029–3056, Sep. 2015.

[18] J. Eisenbeis, T. Mahler, P. R. López, and T. Zwick, "Channel estimation method for subarray based hybrid beamforming systems employing sparse arrays," *Progress Electromagn. Res. C*, vol. 87, pp. 25–38, Aug. 2018.

[19] *Technical Specification Group Services and System Aspects; Release 15 Description; Summary of Rel-15 Work Items (Release 15), V15.0.0 (2019-09)*, 3rd Generation Partnership Project, Sophia Antipolis, France, Sep. 2019.

[20] M. Morelli, C.-C. J. Kuo, and M.-O. Pun, "Synchronization techniques for orthogonal frequency division multiple access (OFDMA): A tutorial review," *Proc. IEEE*, vol. 95, no. 7, pp. 1394–1427, Jul. 2007.

[21] T. Hwang, C. Yang, G. Wu, S. Li, and G. Y. Li, "OFDM and its wireless applications: A survey," *IEEE Trans. Veh. Technol.*, vol. 58, no. 4, pp. 1673–1694, May 2009.

[22] X. Gao, L. Dai, S. Han, I. Chih-Lin, and R. W. Heath, "Energy-efficient hybrid analog and digital precoding for mmwave MIMO systems with large antenna arrays," *IEEE J. Sel. Areas Commun.*, vol. 34, no. 4, pp. 998–1009, Apr. 2016.

[23] J. Eisenbeis *et al.* (Jul. 2020). *Hybrid Beamforming Analysis Based on MIMO Channel Measurements at 28 GHz.* [Online]. Available: https://doi.org/10.36227/techrxiv.12639467.v1

[24] J. Eisenbeis *et al.* (Jul. 2020). *MIMO Communication Measurements in Small Cell Scenarios at 28 GHz.* [Online]. Available: https://doi.org/10.36227/techrxiv.12639740.v1